

Direct growth of carbon microfibres on SiO₂ particles by chemical vapour deposition from ethanol

Feng Wang , Xiaofang Qin, Lixia Yang, Shanmin Gao, Qingyao Wang, Zhenglong Yang

School of Chemistry and Materials Science, Ludong University, Yantai 264025, People's Republic of China

✉ E-mail: wf200818@126.com

Published in Micro & Nano Letters; Received on 1st January 2018; Revised on 29th May 2018; Accepted on 21st June 2018

Carbon microfibres (CMFs) were synthesised on SiO₂ particles by catalytic chemical vapour deposition at 1200°C using ethanol as carbon precursor, iron nitrate as the catalyst precursor, and nitrogen as a carrier gas. The structure and morphology of the products were characterised by X-ray diffraction, scanning electron microscopy, high-resolution transmission electron microscopy and Raman spectroscopy. CMFs obtained after a deposition time of 5 h have a diameter of 5–10 μm and a length of a few hundred micrometres. In the deposition process, Fe–Si–O–C droplets were first formed on the surface of SiO₂ particles, and then carbon fibres grew as a result of the catalysis of the droplets. Carbon fibres have the higher graphitic structures when the deposition process is conducted at 1200°C.

1. Introduction: Since the landmark paper on carbon nanotubes (CNTs) was reported by Iijima in 1991 [1], carbon and carbon-based materials have received wide attention owing to their excellent physical, chemical, mechanical, electrical, thermal and optical properties [2–9]. As a result, many methods have been proposed to synthesise carbon materials with the different morphologies. For example, Ma *et al.* [10] reported the synthesis of centimetre-size multi-branched tree-like carbon structures by the catalytic chemical vapour deposition (CCVD) of toluene using ferrocene as the catalyst precursor. Wang *et al.* [11] prepared well-aligned freestanding arrays of mesoporous carbon nanofibres on silicon wafers using non-ionic triblock copolymer F127 as a soft template and anodic aluminium oxide membranes as hard templates. Qi *et al.* [12] fabricated CNTs with various helical structures by means of catalytic pyrolysis of acetylene at 450°C over Fe nanoparticles prepared by a coprecipitation/reduction method. Xiao *et al.* [13] obtained carbon sheets composed of two layer planes by an easy solvothermal process at 600°C for 12 h. In addition, Wang *et al.* [14] generated helical carbon nanofibre by the pyrolysis of acetylene using Cu nanoparticle catalyst. Mehraban *et al.* [15] synthesised carbon spheres in the presence of cobalt–silicon–mesoporous aluminium silicate by chemical vapour deposition (CVD) using C₂H₂ as the source of carbon at 850°C. In the preparation of carbon materials, CVD is the main synthesis method with a variety of metal catalysts, such as Fe, Ni, Mg, Zn, Sn and their alloys.

In this work, we present a simple and economical thermal CCVD process to synthesise CMFs on SiO₂ particles at 1200°C using ethanol as a carbon precursor. The graphitisation of carbon phase in SiO₂-C composites was confirmed by Raman spectrometry.

2. Experimental procedure

2.1. Preparation of carbon microfibres (CMFs): All chemical reagents were of analytical grade and used without further purification. Firstly, the silica xerogel was prepared by a sol–gel method using tetraethoxysilane as the silica source. An alumina boat with silica xerogel was placed in the centre of a horizontal alumina tube furnace and heated to 1200°C in the air to obtain SiO₂ particles. At the same time, 3.0 g iron nitrate (Fe(NO₃)₃·9H₂O) was dissolved in absolute ethanol (100 ml) under stirring. Then ethanol vapour and iron nitrate were introduced into an alumina tube furnace by a carrier gas of nitrogen with a flow rate of 400 ml/min. Carbon fibres grew on the surface of

SiO₂ particles during the deposition. After a deposition time of 5 h, the carrier gas and power were turned off. The system was cooled down to room temperature naturally under the protection of nitrogen. Finally, CMFs were obtained on SiO₂ particles.

2.2. Characterisation of CMFs: The crystalline phase of the products was characterised by X-ray powder diffraction (XRD) with a Rigaku D/max2500VPC diffractometer using CuKα radiation. The morphology and structure of the products were examined by scanning electron microscopy (SEM, JSM-5610LV) and high-resolution transmission electron microscopy (HRTEM, JEM-2010). Raman spectrometry analysis was recorded to characterise the structure of the carbon phase using a LabRAM HR800 spectrometer (Horiba Jobin Yvon Corp., France, λ = 632.8 nm).

3. Results and discussion: Fig. 1 shows the optical photographs of the products on SiO₂ particles after a deposition time of 5 h. Fig. 1a shows an overview of the products in an alumina boat. From the figure, it can be seen that there are black products on the surfaces of SiO₂ particles. This shows that carbon has been deposited on the surfaces of SiO₂ particles. Fig. 1b reveals a high magnification optical photograph of the products marked with white frame in Fig. 1a. It can be seen that there are many carbon fibres on SiO₂ particles. The growth direction of carbon fibres is in good agreement with the flow direction of carrier gas. This displays carbon fibres grown along the flow direction of ethanol vapour and iron nitrate.

The XRD patterns of the SiO₂ particles obtained before and after the deposition from ethanol are shown in Fig. 2. From Fig. 2a, it can be seen that SiO₂ particles have a very good crystalline phase structure, and all the diffraction peaks can be indexed as a pure cristobalite SiO₂ phase (JCPDS Card No. 39-1425) [16]. After a deposition time of 5 h, the diffraction peaks of the SiO₂ particles become obviously weaker as shown in Fig. 2b. A new diffraction peak at about 2θ = 26° is also found in the XRD pattern. It can be indexed as the characteristic diffraction peak of carbon. This shows that the formation of carbon fibres on SiO₂ particles. In addition, a very weak diffraction peak corresponding to Fe₃C can be formed at 2θ = 43° as a result of carbon atoms dissolution in iron during carbon fibre growth [17, 18]. To imply further the formation of carbon fibres, the sample was treated by HF to get rid of SiO₂. Fig. 2c shows the XRD pattern of the sample treated by HF.

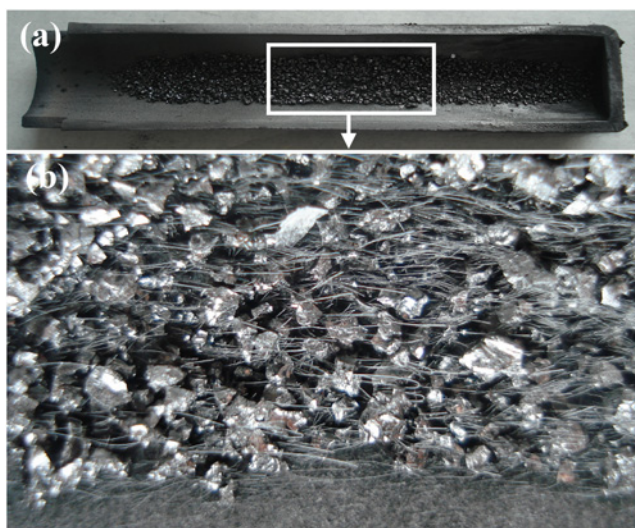


Fig. 1 Optical photographs of the products on SiO₂ particles after a deposition time of 5 h shows
a Formation of carbon
b Growth of carbon fibres on SiO₂ particles

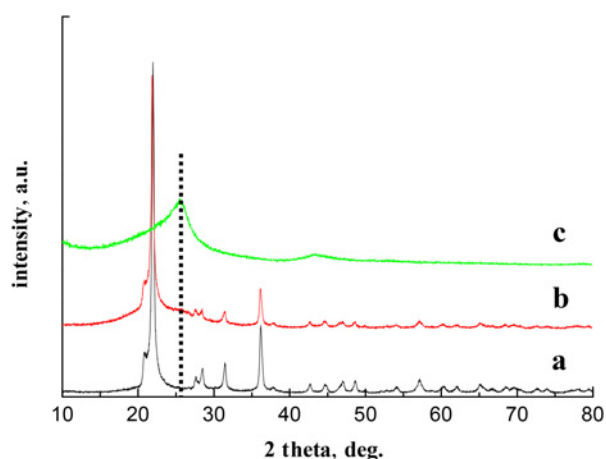


Fig. 2 XRD patterns of the samples obtained before and after the deposition from ethanol
a Before the deposition
b After the deposition
c After the deposition and treated by HF

Strong peaks at $2\theta = 25.7^\circ$ and 43.2° are clearly visible thanks to the (002) and (100) planes of graphite carbon [3, 19], respectively.

The SEM images of carbon fibres are shown in Fig. 3. Figs. 3*a* and 3*b* reveal the growth of carbon fibres on a SiO₂ particle. From the images, it can be seen that many carbon fibres grew on the surfaces of the SiO₂ particle. The high magnification SEM image of carbon fibres is shown in Fig. 3*c*, the image shows the carbon fibres have a diameter of 5–10 μm and a length of a few hundred micrometres. The surfaces of the fibres are not smooth and have a wavy structure. As shown in Fig. 3*d*, there are a large number of droplets (spherical nodules) on the surfaces of SiO₂ particles. The corresponding EDS spectrum (Fig. 3*e*) shows that the droplets mainly consist of Fe, Si, O and C elements, which is also in good agreement with the XRD result. Then these droplets serve as catalyst active points for the direct growth of CMFs on the surfaces of SiO₂ particles. The possible formation process of the carbon fibres can be described as follows. In the initial stage of deposition, C and Fe from the decomposing of ethanol and iron nitrate are deposited on the surfaces of SiO₂ particles to form the Fe–Si–O–C droplets at the high reaction temperature (1200°C). The Fe–Si–O–C droplets

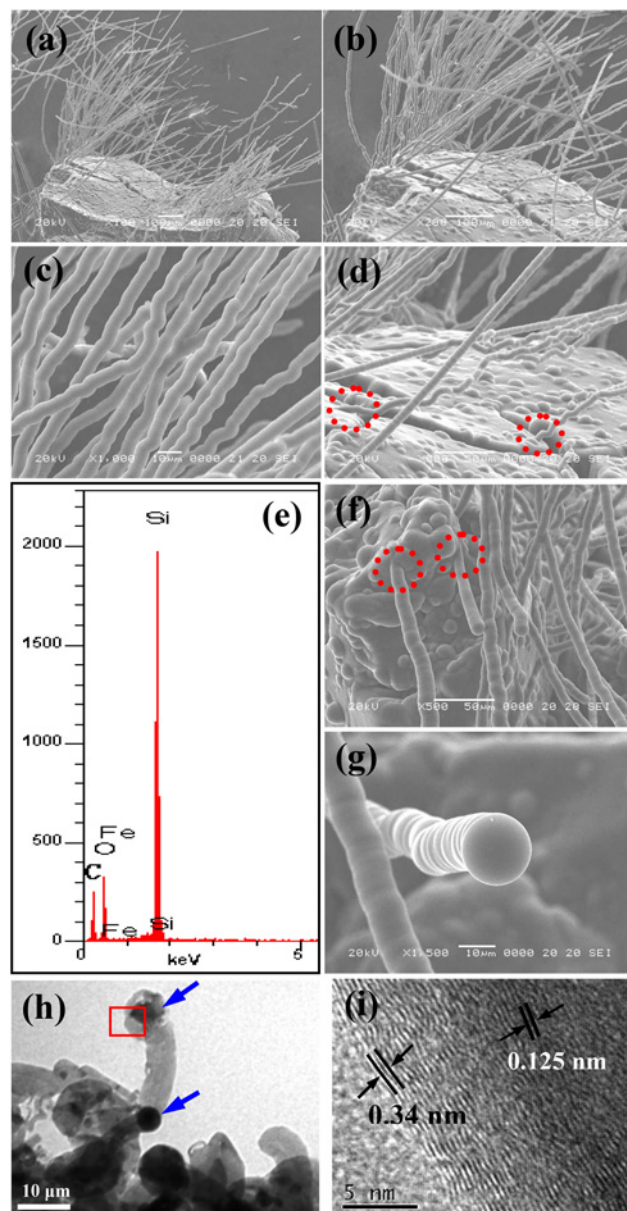


Fig. 3 SEM and HRTEM images of CMFs prepared on SiO₂ particles by CCVD from ethanol

a, b SEM images of CMFs grown on a SiO₂ particle
c High magnification SEM image of carbon fibres
d SEM images of a large number of droplets (spherical nodules) on the surfaces of SiO₂ particles
e EDS spectrum of the droplets
f SEM image of the direct growth of CMFs marked with red circles
g SEM image of the top of a carbon fibre with a spherical and smooth structure
h TEM image of the alloy droplets with core-shell structure
i HRTEM image of the red rectangle region in (h)

continually absorb carbon atoms from the ambience with the deposition. After the concentrations of carbon atoms in the droplets approach saturation, carbon precipitates from the droplets. With the extension of the reaction time, carbon fibres are formed. The direct growth of CMFs marked with red circles on the surfaces of SiO₂ particles was shown in Figs. 3*d* and 3*f*. The SEM image of the top of a carbon fibre is shown in Fig. 3*g*. It is found that the top end of carbon fibre has a spherical structure with the smooth surface, which is agreement with the morphology of the droplets on the surfaces of SiO₂ particles. The structure of the droplets was further characterised by HRTEM. Fig. 3*h* displays a TEM image of the droplets marked with blue arrows. The TEM image clearly shows

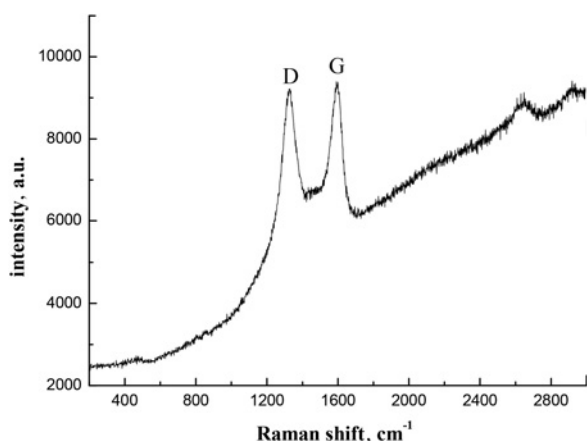


Fig. 4 Raman spectrum of CMFs prepared on SiO₂ particles by thermal CCVD from ethanol

that the droplets have core-shell structure. Fig. 3*i* shows the HRTEM image of the red rectangle region in Fig. 3*h*. From the image, the spacing of the shell between two adjacent fringes is 0.34 nm, which is consistent with the (002) plane of graphitic carbon [20]. The inter-lattice distance of the core is calculated to be 0.125 nm, which is in good agreement with that of Fe₃C (322) planes [21]. These results prove that the direct growth of CMFs is practical on the surfaces of SiO₂ particles with the deposition from ethanol.

Raman spectroscopy was employed to examine the graphitisation of the amorphous carbon phase in the SiO₂/C composites. Fig. 4 presents the Raman spectrum of carbon microfibers prepared on SiO₂ particles by thermal CCVD from ethanol. The two typical peaks located at 1328 and 1598 cm⁻¹ were registered as the D and G bands of carbon, respectively. The D and G bands represented disordered carbon and graphite, respectively. The G band, corresponding to the scattering of the E_{2g} mode (stretching vibrations) observed for sp² domains, is characteristic for graphitic sheets, whereas the D band can be assigned to the scattering of the A_{1g} mode associated with sp³-bonded disorder carbon [18, 22, 23]. The intensity ratio of the D to G bands (I_D/I_G) provides useful information for comparing the degree of graphitisation of various carbon materials, and the ratio of I_D/I_G is smaller, the degree of ordering of the carbon material is higher [24, 25]. In addition, the second-order Raman peaks in the range from about 2500 to 3000 cm⁻¹ are visible in this figure, which is consistent with the 2D peaks of graphite including graphene [5, 26]. In our experiment, a lower I_D/I_G value (0.83) indicated that a dominant graphitic carbon structure is developed at the deposition temperature of 1200°C.

4. Conclusions: In conclusion, CMFs have been synthesised on SiO₂ particles by thermal CCVD from ethanol. CMFs have a diameter of 5–10 μm and a length of a few hundred micrometres. During the deposition, Fe–Si–O–C droplets were first formed on the surface of SiO₂ particles, and then carbon fibres grew as a result of the catalytic activity of the Fe–Si–O–C droplets. The graphitic structures are developed at the deposition temperature of 1200°C.

5. Acknowledgments: This work was financially supported by the National Natural Science Foundation of China (grant no. 51673090), the Science and Technology Development Plan Project of Shandong Province (grant no. 2014GSF117015), the Key Laboratory of Magnetic Molecules & Magnetic Information Materials Ministry of Education, Shanxi Normal University (grant no. 050202040077).

6 References

- [1] Iijima S.: ‘Helical microtubes of graphitic carbon’, *Nature*, 1991, **354**, pp. 56–58
- [2] Saranya K., Subramania A., Sivasankar N.: ‘Influence of earth-abundant bimetallic (Fe-Ni) nanoparticle-embedded CNFs as a low-cost counter electrode material for dye-sensitized solar cells’, *RSC Adv.*, 2015, **5**, pp. 43611–43619
- [3] Wu X.L., Chen L.L., Xin S., *ET AL.*: ‘Preparation and Li storage properties of hierarchical porous carbon fibers derived from alginic acid’, *ChemSusChem*, 2010, **3**, pp. 703–707
- [4] Liu Y., Xu L., Liu J.S., *ET AL.*: ‘Graphene oxides cross-linked with hyperbranched polyethylenimines: preparation, characterization and their potential as recyclable and highly efficient adsorption materials for lead(II) ions’, *Chem. Eng. J.*, 2016, **285**, pp. 698–708
- [5] Musiol P., Szatkowski P., Gubernat M., *ET AL.*: ‘Comparative study of the structure and microstructure of PAN-based nano- and micro-carbon fibers’, *Ceram. Inter.*, 2016, **42**, pp. 11603–11610
- [6] Shang Y.Y., Wang Y., Li S.H., *ET AL.*: ‘High-strength carbon nanotube fibers by twist-induced self-strengthening’, *Carbon*, 2017, **119**, pp. 47–55
- [7] Dai Y.J., Zhang K.X., Li J.J., *ET AL.*: ‘Adsorption of copper and zinc onto carbon material in an aqueous solution oxidized by ammonium peroxydisulphate’, *Sep. Purif. Technol.*, 2017, **186**, pp. 255–263
- [8] Li A., Wang J.J., Dong C., *ET AL.*: ‘Core-sheath structural carbon materials for integrated enhancement of thermal conductivity and capacity’, *Appl. Energy*, 2018, **217**, pp. 369–376
- [9] Jin R.C., Jiang H., Sun Y.X., *ET AL.*: ‘Fabrication of NiFe₂O₄/C hollow spheres constructed by mesoporous nanospheres for high-performance lithium-ion batteries’, *Chem. Eng. J.*, 2016, **303**, pp. 501–510
- [10] Ma H.L., Su D.S., Achim K.H., *ET AL.*: ‘Morphologies and microstructures of tree-like carbon produced at different reaction conditions in a CVD processes’, *Carbon*, 2006, **44**, pp. 2254–2260
- [11] Wang K.X., Zhang W.H., Phelan R., *ET AL.*: ‘Direct fabrication of well-aligned free-standing mesoporous carbon nanofiber arrays on silicon substrates’, *J. Am. Chem. Soc.*, 2007, **129**, pp. 13388–13389
- [12] Qi X.S., Zhong W., Deng Y., *ET AL.*: ‘Synthesis of helical carbon nanotubes, worm-like carbon nanotubes and nanocoils at 450°C and their magnetic properties’, *Carbon*, 2010, **48**, pp. 365–376
- [13] Xiao Y., Liu Y.L., Yuan D.S.: ‘Preparation and characterization of carbon sheets composed of two layer planes’, *Carbon*, 2008, **46**, pp. 559–561
- [14] Wang G.Q., Kuang S., Zhang W.: ‘Helical carbon nanofiber as a low-cost counter electrode for dye-sensitized solar cells’, *Mater. Lett.*, 2016, **174**, pp. 14–16
- [15] Mehraban Z., Farzaneh F., Dadmehr V.: ‘Catalytic chemical vapour deposition synthesis of carbon spheres’, *Mater. Lett.*, 2009, **63**, pp. 1653–1655
- [16] Wang J.G., Liu S., Ding T., *ET AL.*: ‘Synthesis, characterization, and photoluminescence properties of bulk-quantity β-SiC/SiO_x coaxial nanowires’, *Mater. Chem. Phys.*, 2012, **135**, pp. 1005–1011
- [17] Teong Ooi J.H., Liu W.W., Thota V., *ET AL.*: ‘Synthesis of single-walled carbon nanotubes by chemical vapor deposition using sodium chloride support’, *Physica E*, 2011, **43**, pp. 1011–1014
- [18] Philipp A., Hu Y.S., Antonietti M., *ET AL.*: ‘Hollow Fe-containing carbon fibers with tubular tertiary structure: preparation and Li-storage properties’, *J. Mater. Chem.*, 2009, **19**, pp. 1616–1620
- [19] Zhang M.Y., Shao C.L., Mu J.B., *ET AL.*: ‘Hierarchical heterostructures of Bi₂MoO₆ on carbon nanofibers: controllable solvothermal fabrication and enhanced visible photocatalytic properties’, *J. Mater. Chem.*, 2012, **22**, pp. 577–584
- [20] Wu A.B., Yang X.W., Yang H.: ‘Magnetic properties of carbon coated Fe, Co, Ni nanoparticles’, *J. Alloys Compd.*, 2012, **513**, pp. 193–201
- [21] Su J., Gao Y.H., Han X.Y., *ET AL.*: ‘Fe- and Fe₃C-filled carbon nanotube-aligned arrays and flower-like carbon nanostructured clusters with a high coercivity’, *Micro Nano Lett.*, 2012, **7**, pp. 271–274
- [22] Zhang P., Shao C.L., Zhang Z.Y., *ET AL.*: ‘In situ assembly of well-dispersed Ag nanoparticles (AgNPs) on electrospun carbon nanofibers (CNFs) for catalytic reduction of 4-nitrophenol’, *Nanoscale*, 2011, **3**, pp. 3357–3363

- [23] Zeng L.Y., Wang W.B., Lei D., *ET AL.*: 'The effect of carbon micro-fiber substrate pretreatment on the growth of carbon nanomaterials', *Carbon*, 2008, **46**, pp. 359–364
- [24] Wu Y.Z., Reddy M.V., Chowdari B.V.R., *ET AL.*: 'Ramakrishna, long-term cycling studies on electrospun carbon nanofibers as anode material for lithium ion batteries', *ACS Appl. Mater. Interfaces*, 2013, **5**, pp. 12175–12184
- [25] Abouali S., Garakani M.A., Zhang B., *ET AL.*: 'Electrospun carbon nanofibers with in situ encapsulated Co_3O_4 nanoparticles as electrodes for high-performance supercapacitors', *ACS Appl. Mater. Interfaces*, 2015, **7**, pp. 13503–13511
- [26] Pimenta M.A., Dresselhaus G., Dresselhaus M.S., *ET AL.*: 'Studying disorder in graphite-based systems by Raman spectroscopy', *Phys. Chem. Chem. Phys.*, 2007, **9**, pp. 1276–1291